NEUROSCIENCE
RESEARCH ARTICLE
A. M. Kelly, A. W. Seifert / Neuroscience 468 (2021) 16–28

Distribution of Vasopressin and Oxytocin Neurons in the Basal Forebrain and Midbrain of Spiny Mice (*Acomys cahirinus*)

Aubrey M. Kelly [a]* **and Ashley W. Seifert** [b]

[a] *Department of Psychology, Emory University, 36 Eagle Row, Atlanta, GA 30322, USA*

[b] *Department of Biology, University of Kentucky, 675 Rose Street, Lexington KY 40508, USA*

Abstract—The nonapeptides vasopressin (VP) and oxytocin (OT) are present in some form in most vertebrates. VP and OT play critical roles in modulating physiology and are well-studied for their influences on a variety of social behaviors, ranging from affiliation to aggression. Their anatomical distributions have been mapped for numerous species across taxa, demonstrating relatively strong evolutionary conservation in distributions throughout the basal forebrain and midbrain. Here we examined the distribution of VP-immunoreactive (-ir) and OT-ir neurons in a gregarious, cooperatively breeding rodent species, the spiny mouse (*Acomys cahirinus*), for which nonapeptide mapping does not yet exist. Immunohistochemical techniques revealed VP-ir and OT-ir neuronal populations throughout the hypothalamus and amygdala of males and females that are consistent with those of other rodents. However, a novel population of OT-ir neurons was observed in the median preoptic nucleus of both sexes, located dorsally to the anterior commissure. Furthermore, we found widespread sex differences in OT neuronal populations, with males having significantly more OT-ir neurons than females. However, we observed a sex difference in only one VP cell group – that of the bed nucleus of the stria terminalis (BST), a VP neuronal population that exhibits a phylogenetically widespread sexual dimorphism. These findings provide mapping distributions of VP and OT neurons in *Acomys cahirinus*. Spiny mice lend themselves to the study of mammalian cooperation and sociality, and the nonapeptide neuronal mapping presented here can serve as a basic foundation for the study of nonapeptide-mediated behavior in a group of highly social rodents.

Key words: vasopressin, oxytocin, hypothalamus, social behavior, neuropeptide.

*Corresponding author.
E-mail address: aubrey.kelly@emory.edu (A. M. Kelly).

Abbreviations: AC, anterior commissure; ACA, anterior part of anterior commissure; ACP, posterior part of anterior commissure; AH/AHA, anterior hypothalamic area; AHC, anterior nucleus of hypothalamus, central part; AHN, anterior nucleus of hypothalamus; AHP, anterior nucleus of hypothalamus, posterior part; Arc, arcuate nucleus of hypothalamus; AVPe, anteroventral periventricular nucleus; BSTM, medial part of the bed nucleus of the stria terminalis; BSTMPL, posterolateral part of the bed nucleus of the stria terminalis; BSTMPM, posteromedial part of the bed nucleus of the stria terminalis; CA1, field CA1 of the hippocampus; CA2, field CA2 of the hippocampus; CA3, field CA3 of the hippocampus; cc, corpus callosum; cg, cingulum; Cir, circular nucleus of the anterior hypothalamus; Cpu, caudate putamen; D3V, dorsal 3rd ventricle; DG, dentate gyrus; f, fornix; fi, fimbria of the hippocampus; GrDG, granular layer of dentate gyrus; ic, internal capsule; LA, lateroanterior hypothalamic nucleus; LH, lateral hypothalamic area; LPO, lateral preoptic area; LSD, lateral septal nucleus, dorsal part; LV, lateral ventricle; MCPO, magnocellular preoptic nucleus; MeA, medial amygdala; MnPO, median preoptic nucleus; MPA, medial preoptic area; MPO, medial preoptic nucleus; MPOC, medial preoptic nucleus, central part; MPOL, medial preoptic nucleus, lateral part; MPOM, medial preoptic nucleus, medial part; mt, mammillothalamic tract; ns, nigrostriatal fibers; opt, optic tract; ox, optic chasm; PaAP, paraventricular nucleus of the hypothalamus, anterior parvicellular; PaDC, paraventricular nucleus of the hypothalamus, dorsal cap; PaLM, paraventricular nucleus of the hypothalamus, lateral magnocellular; PaMM, paraventricular nucleus of the hypothalamus, medial magnocellular; PaPo, paraventricular nucleus of the hypothalamus, posterior part; PaV, paraventricular nucleus of the hypothalamus, ventral part; Pe, periventricular nucleus of the hypothalamus; PVN, paraventricular nucleus of the hypothalamus; SCh, suprachiasmatic nucleus; SChDM, suprachiasmatic nucleus, dosromedial part; SChVL, suprachiasmatic nucleus, ventrolateral part; Sfi, septofimbrial nucleus; sm, nucleus stria medullaris; SO/SON, supraoptic nucleus; sox, supraoptic decussation; SPa, subparaventricular zone; st, stria terminalis; TS, triangular septal nucleus; ZI, zona incerta.

https://doi.org/10.1016/j.neuroscience.2021.05.034
0306-4522/

INTRODUCTION

The nonapeptides are evolutionarily conserved across vertebrates and modulate basic physiology as well as play phylogenetically widespread roles in the modulation of various behaviors, including affiliation, bonding, parental behavior, anxiety-like behavior, and aggression (Donaldson and Young, 2008; Goodson and Thompson, 2010; Bosch, 2011; Albers, 2012). Nonapeptide distributions have been described for many species, demonstrating that these peptides arise primarily from magnocellular and parvocellular cell populations in the hypothalamus and preoptic area that produce: arginine vasotocin (Ile^3-VP) in non-mammalian vertebrates and arginine vasopressin (Arg^8-VP) in mammals; isotocin (Ser^4, Ile^8-OT) in bony fishes, mesotocin (Ile^8-OT) in lobe-finned fishes, birds, reptiles, amphibians, and some marsupials, and oxytocin (Leu^8-OT) in most eutherian mammals (Acher

and Chauvet, 1995; Hoyle, 1998; Lee et al., 2011). Although the nomenclature is taxon-specific, all jawed vertebrates express single forms of VP and OT, and thus, we refer to all forms of the nonapeptides as VP and OT for ease of communication (Kelly and Goodson, 2014c). In addition to the primary VP and OT populations in the preoptic area and hypothalamus, there are also several other smaller hypothalamic and extrahypothalamic nonapeptide cell groups where species and sex differences are more likely to be observed. While most reptiles, birds, and mammals exhibit an average of 8–10 distinct VP and OT cell groups, there can be considerable variation (Moore and Lowry, 1998). For example, some amphibians (e.g., roughskin newts) exhibit up to 19 distinct VP neuronal populations (Lowry et al., 1997) and 23 different brain areas produce OT in mustached bats (Prasada Rao and Kanwal, 2004). Because of this variation, it is important to characterize nonapeptide distributions in a species prior to examining nonapeptide-mediated behavior.

VP and OT peptide producing neuronal populations have been characterized for several species of rodents, including laboratory rats (Dogterom et al., 1978; DiBenedictis et al., 2017) and mice (Rood and De Vries, 2011; Otero-Garcia et al., 2016), tree shrews (Ni et al., 2014), eusocial mole rats (Rosen et al., 2008; Valesky et al., 2012), African striped mice (Schoepf et al., 2015), several species of hamster (Dubois-Dauphin et al., 1990; Whitman and Albers, 1998; Shi and Bartness, 2000; Wang et al., 2013), and multiple species of gerbils (Yu et al., 2020) and voles (Wang et al., 1996; Qiao et al., 2014). Despite the availability of numerous rodents for social neuroscience studies, there are surprisingly few species that live in large groups and do not exhibit eusociality. To our knowledge, African striped mice (*Rhabdomys pumilio*), which can be found in groups of up to 30 mixed-sex individuals (Schradin et al., 2020), are among the few rodents tractable for laboratory studies that exhibit larger group living, whereas the other species listed above are territorial or live in small family groups. Although prairie voles and Mongolian gerbils are often used for the study of prosocial behaviors, both species exhibit aggression when interacting with novel, same-sex conspecifics (Lee et al., 2019; Pan et al., 2020). In order to expand the species available for the study of neural mechanisms underlying grouping behaviors, here we aim to characterize the distribution of nonapeptide-producing neurons in the highly social spiny mouse *Acomys cahirinus*.

Despite being referred to as a mouse, phylogenetic and molecular studies place *Acomys* within the Deomyinae, a distinct subfamily within the Murinae that are more closely related to Gerbillinae (gerbils) than mice (Fabre et al., 2012; Alhajeri et al., 2015; Steppan and Schenk, 2017). Historically, spiny mice were studied for their propensity to develop type II diabetes (Gonet et al., 1966; Shafrir, 2000), but more recently they have become an exciting model to study complex tissue regeneration (Seifert et al., 2012; Gawriluk et al., 2016). In addition to their remarkable regenerative ability, at least one species (*A. cahirinus*) exhibits a menstrual cycle in captivity (Bellofiore et al., 2017) and have become an emerging model for human-like reproductive biology (Bellofiore et al., 2018). As murid rodents they are unique in their precocial mode of development, with in utero development lasting 38–42 days depending on the species (Brunjes, 1990; Haughton et al., 2016). Their extended embryonic development compared to mice and rats has provided researchers an opportunity to study neural and glial developmental postnatal growth patterns (Brunjes, 1985; Brunjes et al., 1989).

Spiny mice are found throughout Africa, the Middle East, and southern Asia. They are communal breeders that dwell in crevices and rocky outcroppings (Nowak, 1999; Deacon, 2009; Frynta et al., 2011). Although social behavior has not been extensively studied in spiny mice, preliminary data from our lab and studies from other labs suggest that spiny mice are highly social and that both males and females engage in positive interactions with conspecifics in numerous contexts. Studies examining the communal breeding of *Acomys dimidiatus* have shown that kinship and familiarity have no effect on alloparental care, such that care is directed toward any pup and lactating females will nurse pups regardless of genetic relation (Tuckova et al., 2016). This high degree of prosociality was also demonstrated in a study that found that established spiny mouse breeding groups will accept newcomers, displaying low levels of aggression (Cizkova et al., 2011). Early studies from our lab have found that male and female spiny mice are highly affiliative in non-reproductive contexts, and exhibit little to no aggression with familiar individuals or unrelated, same-sex conspecifics (Kelly et al. *unpub obs*.). Furthermore, in the laboratory, spiny mice can be group housed in cages of 10–20 same-sex, mixed relation individuals and are highly interactive (Haughton et al., 2016). Together, these findings suggest that spiny mice (specifically *A. cahirinus*) may be an excellent organism for studying the mechanisms of reproductive and non-reproductive sociality. Given that the nonapeptides promote affiliative behaviors in numerous species (Donaldson and Young, 2008; Kelly and Goodson, 2014c), spiny mice may be especially valuable for understanding nonapeptide-mediated gregariousness and sociality in mammals.

In the present study, we aimed to provide a detailed analysis of distribution of VP- and OT-producing neuronal populations throughout the brains of males and female spiny mice (*A. cahirinus*) via immunohistochemistry. We observed distributions of nonapeptide cell groups in hypothalamic and extrahypothalamic regions that are similar to what has been reported for other rodents. Additionally, we found widespread sex differences in OT, but not VP, cell number. These findings provide a quantitative map of nonapeptide neuronal expression in spiny mice and reveal effects of sex on adult VP and OT neuronal densities.

EXPERIMENTAL PROCEDURES

Animals

Six adult male and six adult female spiny mice (*Acomys cahirinus*) ranging from PND 60–100 were used for the purposes of this study. Spiny mice were obtained from the breeding colony of Dr. Ashley Seifert at the University of Kentucky, Lexington Kentucky USA. All animals were housed in same-sex groups of 10–15 individuals in metal wire cages (24 in. H × 18 in. W × 16 in. D) with floors that were fully filled with pelleted pine bedding. Animals were exposed to natural light corresponding to an approximately 12/12 light dark cycle (brains were harvested in May) and were provided with autoclaved water and a 3:1 mixture by volume of 14% protein mouse chow (Teklad Global 2014, Envigo) and black-oil sunflower seeds (Pennington Seed Inc., Madison, GA) ad libitum. The temperature was maintained at 23 °C with 50% humidity. All procedures were approved by the Institutional Animal Care and Use Committee of the University of Kentucky (Protocol 2019-3254) and Emory University (Protocol 201900126).

Tissue preparation

To visualize VP and OT, subjects were sacrificed by isoflurane overdose and transcardially perfused with 0.1 M phosphate buffered saline (PBS) followed by 4% paraformaldehyde dissolved in 0.1 M borate buffer (pH 9.5). Brains were extracted, post-fixed overnight in 4% paraformaldehyde dissolved in 0.1 M borate buffer (pH 9.5) before cryoprotection in 30% sucrose dissolved in PBS for 48 h. Brains were frozen whole in brain molds containing Tissue-Tek O.C.T. Compound (Sakura Finetek), transported on dry ice to Emory University, and were then stored at −80 °C. Prior to immunohistochemical processing, brains were thawed and sectioned coronally at 40 μm using a cryostat, with every third section being saved for use in the present study.

Western blot characterization of VP and OT antibodies

To confirm that our VP and OT antibodies bind specifically to spiny mouse VP and OT, respectively, we provided fresh frozen whole male and female spiny mouse brains and antibodies to RayBiotech (Atlanta, GA) for auto-western processing. Briefly, total cellular proteins were extracted with protease and phosphate inhibitors. Samples were prepared using a standard boiling procedure with beta-mercaptoethanol and SDS to denature proteins. Samples and reagents were loaded into an assay plate and placed into a capillary immunoassay western machine. A minimum of 40 nL of sample was automatically loaded into the capillary and separated by size as they migrated through a stacking and separation matrix. The separated proteins were then immobilized to the capillary wall via proprietary, photoactivated capture chemistry. Target peptides were identified using the primary antibodies and immunoprobed using HRP-conjugated secondary antibodies.

Primary antibodies submitted for western blot analysis included: (1) guinea pig anti-VP (1:1000; BMA Biomedicals, Switzerland; Catalog # T-5048), (2) rabbit anti-VP (Millipore, Billerica, MA; Catalog #AB1565), (3) mouse anti-OT (3:1000; Millipore, Billerica, MA; Catalog #MAB 5296), and (4) guinea pig anti-OT (1:1000; BMA Biomedicals, Switzerland; Catalog # T-5021). These antibodies were chosen because they are antibodies that we have successfully used in prairie voles (Kelly et al., 2017, 2018a).

Western blots yielded similar results for male and female tissue. Representative results from the western blots run on male tissue are shown in Fig. 1. For the guinea pig anti-VP, we observed a faint band at 2 kilodaltons (kDa; Fig. 1A). The National Institute of Health's (NIH) National Library of Medicine reports the molecular weight of arginine vasopressin as 1028.2 g/mol, or 1.028 kDa (NCfB, 2020b). Additionally, Western blot analysis revealed a dark band at 2 kDa for the mouse anti-OT (Fig. 1B) and the guinea pig anti-OT (Fig. 1C). The NIH's National Library of Medicine reports the molecular weight of oxytocin as 1007.2 g/mol, or 1.007 kDa (NCfB, 2020a). However, for the rabbit anti-VP (Millipore, Billerica, MA; Catalog #AB1565), we observed two dark bands at 2 kDa and 5 kDA (Fig. 1D). Because the rabbit anti-VP yielded two bands, we did not use this antibody for immunohistochemistry.

Antibody characterization

We conducted specificity controls on the primary antibodies that yielded expected molecular weights in the western analyses (e.g., guinea pig anti-VP, mouse anti-OT, and guinea pig anti-OT). Primary antibodies were preadsorped with 50 μM VP (Sigma Aldrich) or 50 μM OT (Sigma Aldrich) at room temperature for 4 h prior to overnight tissue incubation. Immunoreactive staining was eliminated in preadsorped controls. In addition, in order to determine if there is cross-reactivity between VP and OT, we also preadsorped the guinea pig anti-VP in 50 μM OT and the mouse anti-OT and guinea pig anti-OT in 50 μM VP. This did not result in

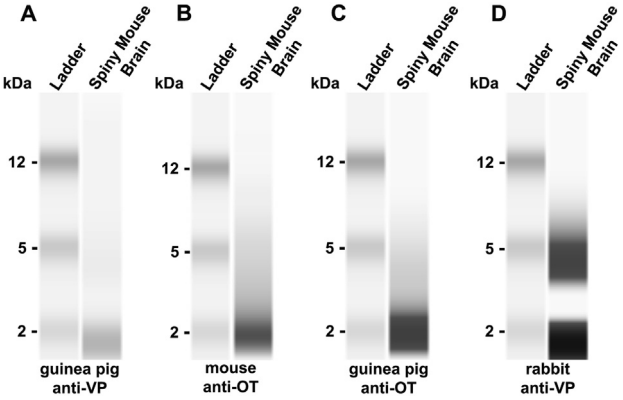

Fig. 1. Western blot characterization of vasopressin and oxytocin antibodies: Western blot of **(A)** guinea pig anti-VP primary antibody, **(B)** mouse anti-OT primary antibody, **(C)** guinea pig anti-OT primary antibody, and **(D)** rabbit anti-VP primary antibody against spiny mouse whole brain protein extract showing bands representing VP and OT, respectively.

reduced staining, indicating low cross-reactivity with VP and OT.

Immunohistochemistry

Tissue was immunofluorescently stained for VP and OT following previously established protocols (Kelly et al., 2011, 2017, 2018a; Kelly and Goodson, 2014a, 2014b). Tissue was rinsed 5× for 10 min in 0.1 M PBS (pH 7.4), incubated for 1 h in a blocking solution (PBS + 10% normal donkey serum + 0.03% Triton-X-100) to prevent non-specific binding, and then incubated for approximately 48 h in primary antibodies diluted in PBS containing 5% normal donkey serum + 0.03% Triton-X-100. Primary antibodies used were guinea pig anti-VP (1:1000; BMA Biomedicals, Switzerland; Catalog # T-5048; RRID:AB_518680) and mouse anti-OT (3:1000; Millipore, Billerica, MA; Catalog #MAB 5296; RRID: AB_2157626). We chose the mouse anti-OT for this study over the guinea pig anti-OT antibody simply due to availability and because it allowed us to double-label cells in one series of tissue. The primary incubation was followed by two 30 min rinses in PBS. Tissue was incubated for 1 h in a biotinylated donkey anti-guinea pig secondary antibody (8:1000; Jackson Immunoresearch, West Grove, PA), rinsed twice for 15 min in PBS, and incubated for 2 h at room temperature in streptavidin conjugated to Alexa Fluor 488 (3:1000) and donkey anti-mouse secondary conjugated to Alexa Fluor 594 (5:1000). All secondary antibodies were diluted in PBS containing 5% normal donkey serum + 0.03% Trion-X-100. Alexa Fluor conjugates were obtained from ThermoFisher Scientific (Waltham, MA). Following two 30 min rinses in PBS, sections were mounted on microscope slides and coverslipped with Prolong Gold antifade containing a DAPI nuclear stain (ThermoFisher Scientific).

Microscopy and artwork

Photomicrographs were obtained using a Zeiss AxioImager II microscope outfitted with an AxioCam MRm, z-drive, and an Apotome optical dissector (Carl Zeiss Inc., Gottingen, Germany). Flattened z-stack images were processed with Zen Pro software (Carl Zeiss Inc., Gottingen, Germany). Images were pseudocolored in order to be colorblind friendly. Designation of neuroanatomical structures was based on Paxinos and Franklin's mouse brain atlas (Paxinos et al., 2009). Representative camera lucida schematics were constructed in Illustrator (Adobe Systems, San Jose, CA) using vector drawings of mouse brain atlas images.

Neural quantification

In two male and two female brains, we examined tissue ranging from the olfactory bulbs through the periaqueductal gray for VP-ir and OT-ir neurons. We observed nonapeptide-ir cells only between the lateral septum (LS) and the ventromedial hypothalamus (VMH), and thus tissue from the remaining four female and four male brains were processed and analyzed from the LS through the VMH. Cell counts were conducted in Photoshop CS6 (Adobe Systems, San Jose, CA) and Image J (National Institutes of Health, Bethesa, MD) as previously described (Kelly et al., 2017). We quantified VP-ir neurons in the BST, suprachiasmatic nucleus (SCN), anterior hypothalamus (AH), PVN, supraoptic nucleus (SON), lateral hypothalamus (LH), and medial amygdala (MeA), and OT-ir neurons in the median preoptic nucleus (MnPO), BST, periventricular nucleus (Pe), AH, PVN, SON, and LH. This was done by counting the total number of VP-ir or OT-ir neurons present in a brain region in two tissue sections, one at a rostral level and another at a caudal level. For the SON and PVN, 200um separated the rostral and caudal levels, whereas 80um separated the rostral and caudal levels for all other nonapeptide cell groups. When there were no significant sex differences between rostral and caudal levels, the total for both levels was used for the box-and-whisker plots. However, all data for rostral, caudal, and combined measurements are presented in tables below.

Statistical analysis

Data were not normally distributed and were therefore analyzed using Mann–Whitney *U* tests. All data were analyzed using SPSS 27 (IBM Analytics, USA), and graphs were made using Prism 8 (GraphPad, USA).

RESULTS

VP-ir staining

In both males and females, we observed VP-ir cells in the BST that originated ventral of the stria terminalis, cascading medially alongside the internal capsule (Fig. 2A; Fig. 3A). Caudally, BST VP-ir neurons clustered between the fornix and anterior commissure (Fig. 2B; Fig. 3B). A small population of VP-ir cells were present in the SCN (Fig. 2B; Fig. 3C). VP-ir cells were present in a tight cluster in the AH (Fig. 2C, D; Fig. 3D), and were found scattered throughout the LH (Fig. 3E). The VP-ir cells of the LH persisted for longer on a rostral-caudal axis than any other VP-ir cell group; these cells appear more lateral when progressing caudally through the brain (Fig. 2C–F). Robust VP-ir cell groups were observed in the PVN and SON (Fig. 2C–F; Fig. 3C and F). The PVN VP-ir population exhibited a trapezoidal shape that increased in size when proceeding caudally through the brain before tapering off. Lastly, VP-ir cells were found in the MeA well after the majority of the SON VP-ir cell group was no longer visible (Fig. 2F; Fig. 3G). Scattered fibers were observed around all VP-ir cell groups, except the SCN, and are represented in Fig. 2.

We observed effects of sex on VP-ir cell densities only in the BST VP neuronal population. While males had more VP-ir cells than females in a combined measurement of both the rostral and caudal BST ($U = 0$, $P < 0.01$; Fig. 4A), this effect of sex was statistically significant only rostrally ($U = 0$, $P < 0.01$; Fig. 4A). This suggests that the effect of sex on overall BST VP-ir cell densities may be driven by differences in

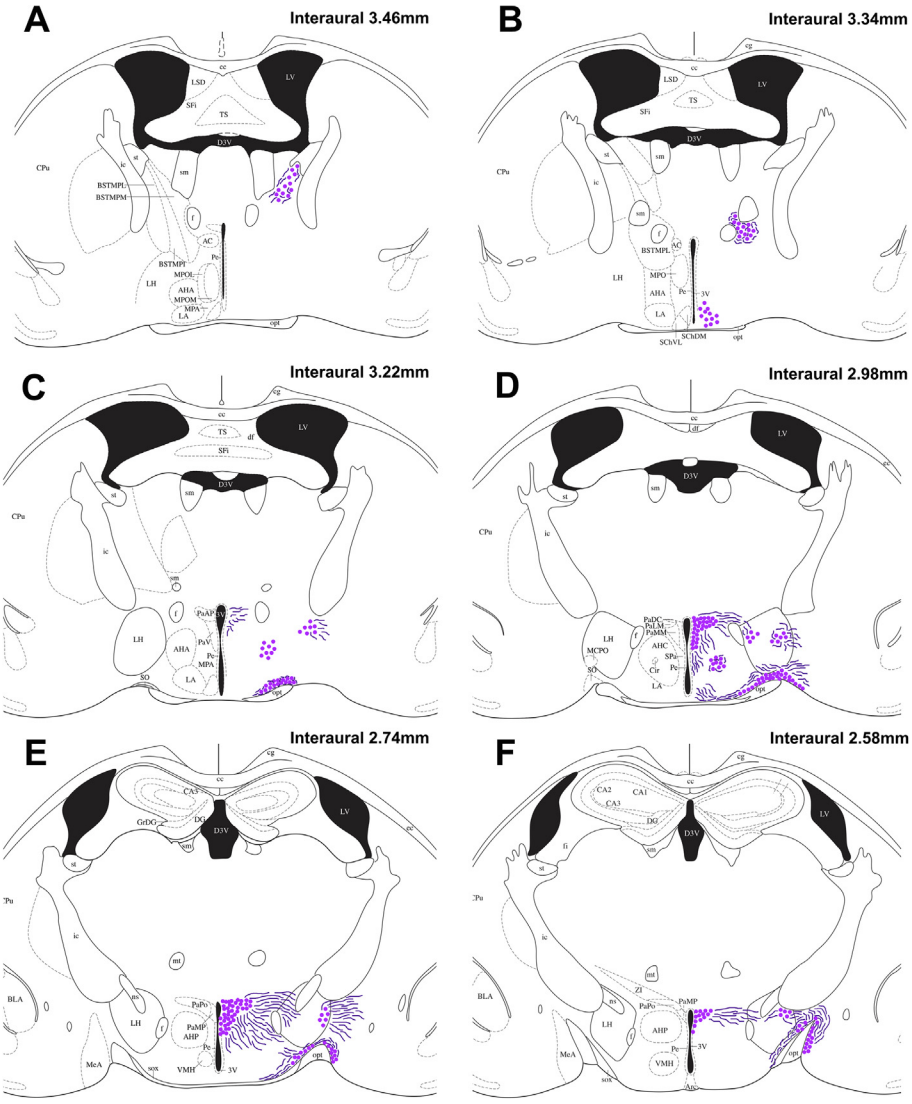

Fig. 2. Distribution of vasopressin-immunoreactive cells and fibers: Camera lucida drawings showing the distribution of VP-ir cells (dots) and observable fibers (lines) in the spiny mouse **(A–F)**. Representative coronal sections are described from rostral to caudal, with reference to interaural line. The majority of the cortex has been cropped to maximize the size of areas containing VP-ir cells. For abbreviations, see Abbreviations.

the rostral part of the cell group. No other VP-ir cell group exhibited sex differences in cell densities (all $P > 0.47$; Fig. 4B, C). For mean densities of VP-ir cell groups, see Table 1.

OT-ir staining

We observed large OT-ir cells in the MnPO, located dorsal of the anterior commissure (Fig. 5A; Fig. 6A). OT-ir cells lined the third ventricle in the Pe (Fig. 5A–C; Fig. 6B), and scattered OT-ir cells were found in the BST (Fig. 5A–C; Fig. 6C) of males only. Additionally, there were scattered OT-ir cells throughout the LH (Fig. 4D–F; Fig. 6D), and we observed a dense cluster of OT-ir in the AH, with the more caudal level clustering around the nucleus circularis (Fig. 5D, E; Fig. 6E, F). Lastly, the PVN and SON exhibited robust OT-ir neuronal populations (Fig. 5D–F; Fig. 6G, H). Scattered fibers were observed around all OT-ir cell groups and are represented in Fig. 5.

We found numerous differences in the number of OT-ir cells between male and females. Compared to females, males exhibited significantly more OT-ir cells in the MnPO ($U = 1$, $P < 0.01$; Fig. 7A), Pe ($U = 0$, $P < 0.01$; Fig. 7A), and LH ($U = 0$, $P < 0.01$; Fig. 7A). Although males exhibited a small population of BST OT-ir cells, this population was absent in females ($U = 0$, $P < 0.01$; Fig. 7A). Furthermore, while males had more OT-ir cells than females in a combined measurement of both the rostral and caudal AH ($U = 0$, $P < 0.01$; Fig. 7B), this effect of sex was statistically significant only rostrally ($U = 0$, $P < 0.01$; Fig. 7B). This suggests that the effect of sex on overall AH OT-ir cell densities may be driven by differences in the rostral part of the cell group. Cell densities in the PVN and SON did not differ between the sexes (all $P > 0.20$). For mean densities of OT-ir cell groups, see Table 2.

DISCUSSION

Here we described the distribution of VP-ir and OT-ir neurons in the fore- and midbrains of male and female spiny mice. Overall, the location of nonapeptide cell groups is similar to what has been reported in other rodents. However, we found widespread effects of sex on OT-ir neuronal densities, with males having significantly more OT-ir neurons than females in all OT cell populations except for those located in the PVN and SON. While some VP-ir and OT-ir fibers were observable in our tissue sections, future studies utilizing viral tracer methods will be used to accurately characterize nonapeptide neuronal axonal projections.

Comparison of vasopressin and oxytocin neuronal populations across rodents

The VP and OT neuronal populations of the PVN and SON were the largest VP-ir and OT-ir cell groups observed in the present study, which is consistent with findings across amniotes (Kelly and Goodson, 2014c). PVN and SON VP and OT modulate basic physiological processes as well as numerous social behaviors such as affiliation, parental care, bonding, social recognition,

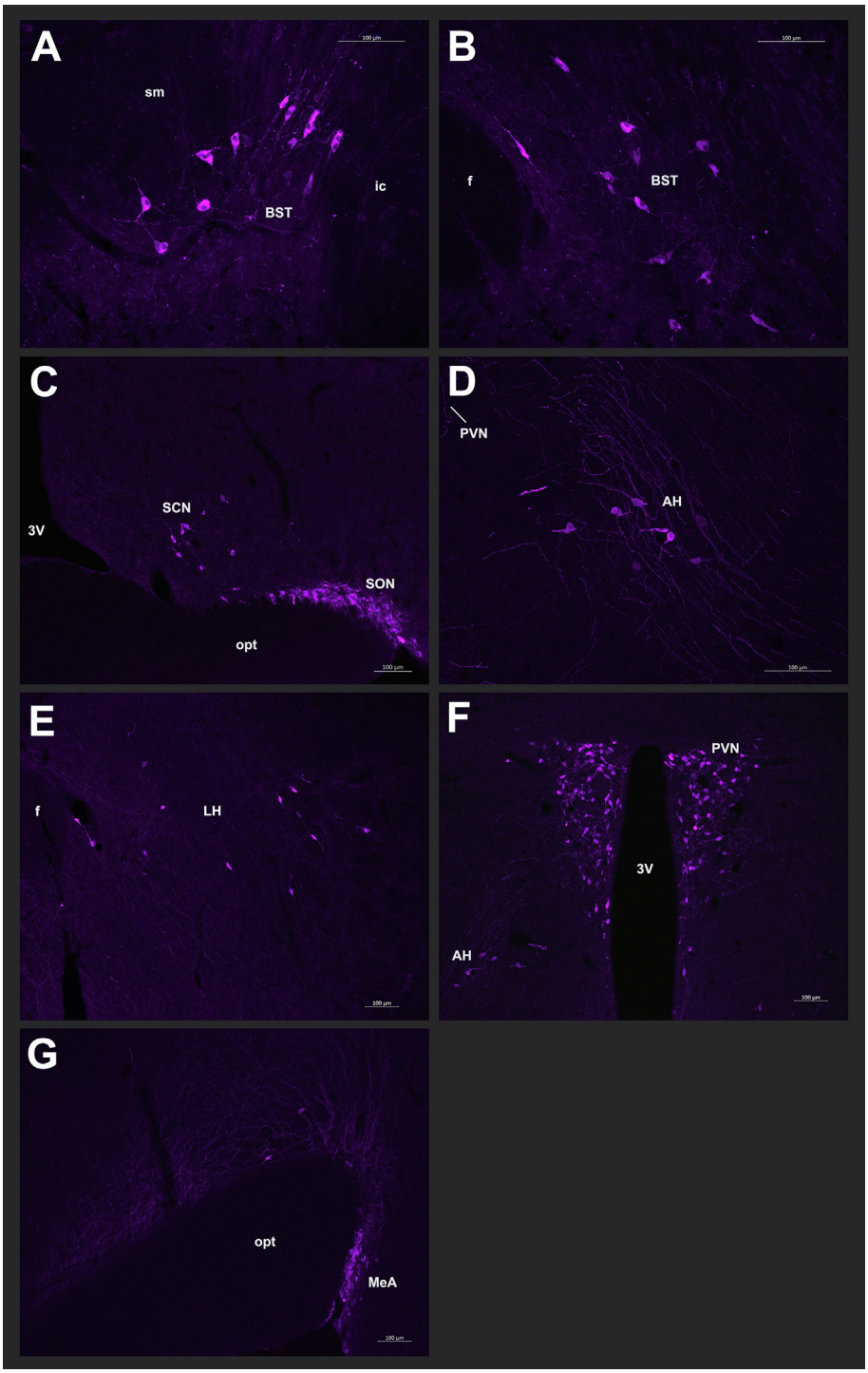

Fig. 3. Photomicrographs of vasopressin-immunoreactive cells: Representative photomicrographs from a male spiny mouse of VP-ir cells in the **(A)** rostral BST (20× magnification), **(B)** caudal BST (20× magnification), **(C)** SCN and SON (10× magnification), **(D)** AH (20× magnification), **(E)** LH (10× magnification), **(F)** PVN (10× magnification), and **(G)** MeA (20× magnification). Images were pseudocolored purple.

and anxiolysis (Landgraf and Neumann, 2004; Donaldson and Young, 2008; Goodson and Thompson, 2010; Kelly and Goodson, 2014c). The presence of nonapeptide neurons in the PVN and SON have been reported for all rodents in which nonapeptide neurons have been described.

Although nonapeptide cell groups of the PVN and SON are well-described across rodents, fewer studies have reported OT-ir cells in the Pe. Here we observed a robust Pe OT-ir cell group in the spiny mice that appears when the anterior commissure is merged and prior to the appearance of the PVN OT-ir cell group. A similarly robust Pe OT population is found in male and female prairie voles (Kelly et al., 2017), pine, montane, and meadow voles (Wang et al., 1996), and CD-1 mice (Otero-Garcia et al., 2016). The functions of the Pe OT cell group are largely unknown, however, a study in prairie voles suggests a potential role for this cell population in parental behavior (Kelly et al., 2017).

One of the most novel findings in the present study is that we observed large OT-ir neurons in the MnPO located dorsal of the anterior commissure. To our knowledge, the presence of MnPO OT neurons has not been reported in any other species. However, OT-ir fibers are present in the MnPO of CD-1 mice and Syrian hamsters (Whitman and Albers, 1998; Otero-Garcia et al., 2016), and VP-ir fibers are found in the MnPO of mice (Rood and De Vries, 2011). The MnPO is important for regulating thirst, sleep, body temperature, and hormone release (McKinley et al., 2015). While the role of OT in the MnPO is currently unknown, this OT neuronal population may be more likely to regulate physiology than social behavior.

As has been reported in other mammals, we observed VP-ir neurons in the SCN. However, compared to photomicrographs of VP-ir cells in the SCN of C57BL/6 mice (Rood and De Vries, 2011), spiny mice exhibit a relatively small VP neuronal population in the SCN. Aside from naked mole rats, which have a complete absence of VP-ir cells in the SCN (Rosen et al., 2007), the presence of VP-ir cells in this region has been reported for several species, including Ansell's mole rats (Valesky et al., 2012), normal rats (Vandesande et al., 1975), and common voles (Van der Zee et al., 1999). The SCN is well known for regulating circadian rhythms (Hastings et al., 2018).

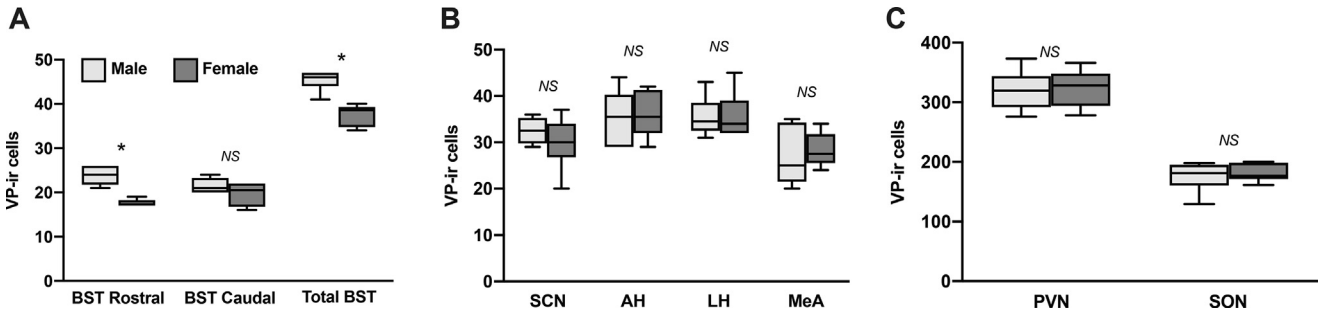

Fig. 4. Effects of sex on the density of vasopressin-immunoreactive cells: Box-and-whisker plots depicting the median, 25th and 75th quartiles, with whiskers showing the 5th and 95th percentile in males (light gray) and females (dark gray) in **(A)** the rostral and caudal portions of the BST, as well as a combined BST measure, **(B)** the SCN, AH, LH, and **(C)** the PVN and SON. *Indicates $P < 0.01$. *NS* indicates not statistically significant.

Table 1. Density of vasopressin immunoreactive cells (mean ± SEM) in the brain of male and female African spiny mice. *Indicates $P < 0.01$. *NS* indicates not statistically significant

Brain region	VP-ir cells		Mann Whitney
	Male	Female	
AH Rostral	16.3 ± 0.8	18.9 ± 1.3	*NS*
AH Caudal	19.0 ± 2.2	17.2 ± 0.8	*NS*
AH Combined	35.3 ± 2.4	36.0 ± 2.0	*NS*
BST Rostral	28.8 ± 0.8	17.8 ± 0.3	*
BST Caudal	21.5 ± 0.7	19.6 ± 1.1	*NS*
BST Combined	45.3 ± 1.0	37.5 ± 1.0	*
LH Rostral	18.9 ± 1.2	19.7 ± 1.7	*NS*
LH Caudal	16.7 ± 1.7	16.0 ± 1.7	*NS*
LH Combined	35.5 ± 1.7	35.6 ± 2.0	*NS*
PVN Rostral	198.8 ± 10.1	196.8 ± 13.3	*NS*
PVN Caudal	121.0 ± 6.0	126.7 ± 6.4	*NS*
PVN Combined	319.8 ± 13.5	323.5 ± 13.0	*NS*
SCN Rostral	13.3 ± 1.0	11.3 ± 0.8	*NS*
SCN Caudal	19.2 ± 1.2	18.5 ± 1.6	*NS*
SCN Combined	32.5 ± 1.3	29.8 ± 2.3	*NS*
SON Rostral	78.7 ± 9.2	83.2 ± 5.9	*NS*
SON Caudal	97.0 ± 5.4	90.0 ± 3.4	*NS*
SON Combined	175.7 ± 10.2	181.2 ± 6.1	*NS*

Interestingly, *Acomys russatus* exhibits flexible sleep patterns and is diurnal in the wild, but nocturnal under laboratory conditions (Fluxman and Haim, 1993; Gutman and Dayan, 2005). It is worth speculating whether the relatively small VP population in *A. cahirinus* is reflective of flexible sleep patterns in spiny mice.

A commonly studied nonapeptide cell group in social neuroscience studies is that of the BST VP neuronal population. Similar to other rodents, the spiny mice exhibit a robust BST VP cell group. VP-ir cells in the BST have been observed in several species of vole (Wang, 1995; Wang et al., 1996), jerboas (Lakhdar-Ghazal et al., 1995), rats (DiBenedictis et al., 2017), mice (Rosen et al., 2006), Mongolian gerbils (Simmons and Yahr, 2011), African striped mice (Schoepf et al., 2015), Syrian hamsters (Albers et al., 1991), and Ansell's mole rats (Valesky et al., 2012). In all of these species, relatively robust VP-ir populations are reported. BST VP is involved in nonreproductive prosocial behaviors in prairie voles (Kelly et al., 2018b), sociosexual behavior in mice (Ho et al., 2010), social investigation in mice (Rigney et al., 2019), and maternal behavior in California mice (Bester-Meredith and Marler, 2012). In addition to VP-ir cells, we also found a few OT-ir cells scattered throughout the BST of male, but not female, spiny mice. Few studies have reported the presence of OT-ir neurons in the BST, however, similar to our observations here, OT-ir cells are present in the BST of Mongolian gerbils (Simmons and Yahr, 2011), prairie voles (Kelly et al., 2017), mice (Otero-Garcia et al., 2016), and mole rats (Rosen et al., 2008; Valesky et al., 2012). Compared to the BST VP cell group, less is known about the contributions of BST OT-ir cells to behavior. However, a recent study in male California mice demonstrated that BST OT knockdown decreased social approach behavior and prevented social stress-induced increases in social vigilance (Duque-Wilckens et al., 2020).

Both VP and OT are produced in the AH of several species, with most species having more VP-ir cells than OT-ir cells in this region. Here we found that spiny mice exhibit robust VP-ir and OT-ir populations in the AH. Similar findings have been reported for Ansell's mole rats (Valesky et al., 2012), greater long-tailed, Syrian, and Chinese hamsters (Jackson et al., 2005; Xu et al.,

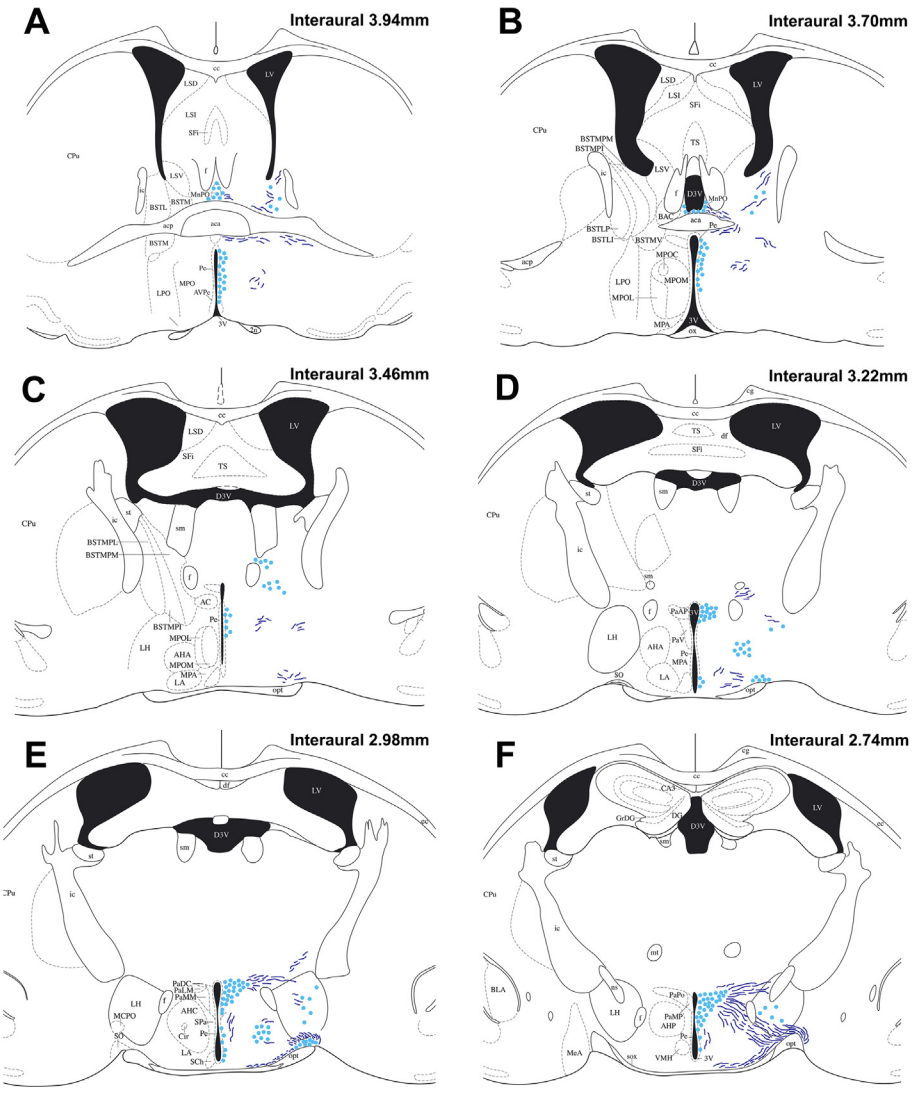

Fig. 5. Distribution of oxytocin-immunoreactive cells and fibers: Camera lucida drawings showing the distribution of OT-ir cells (dots) and observable fibers (lines) in the spiny mouse **(A–F)**. Representative coronal sections are described from rostral to caudal, with reference to interaural line. The majority of the cortex has been cropped to maximize the size of areas containing OT-ir cells. For abbreviations, see Abbreviations.

2010; Wang et al., 2013), and mandarin voles. Whereas, for other species, the AH VP-ir cell group is relatively robust while there is a complete lack of or less than 5 AH OT-ir cells. These species include prairie, meadow, montane, pine, and Brandt's voles (Wang et al., 1996; Xu et al., 2010), jerboas (Lakhdar-Ghazal et al., 1995), mice (Rood and De Vries, 2011; Otero-Garcia et al., 2016), and wild-type and domesticated rats (Ruan and Zhang, 2016). The VP population of the AH has been studied substantially more than OT-ir cells in this region. AH VP is most commonly studied in relation to aggression and has been shown to promote aggression in prairie voles (Gobrogge et al., 2009) and hamsters (Grimes et al., 2007). To our knowledge, extremely few studies have examined the role of AH OT-ir neurons in behavior. However, studies in hamsters that examine the "MPO-AH continuum" have found that OT injected into these regions decreases aggression in females, suggesting that the AH OT neuronal population may have anti-aggressive functional properties (Harmon et al., 2002). An interesting consideration for future studies would be to examine whether the overlapping AH VP and OT cell groups have opposing effects on social behavior. Because spiny mice exhibit robust AH OT and VP populations, they are excellent species for exploring this possibility.

We observed several scattered VP-ir neurons throughout the LH. Similar observations have been described for rats (De Vries et al., 1985), mice (Rood and De Vries, 2011; Otero-Garcia et al., 2016), golden and Chinese hamsters (Dubois-Dauphin et al., 1990; Wang et al., 2013), Ansell's mole rats (Valesky et al., 2012), and prairie voles (Kelly et al., 2017). The functions of LH VP are not well known, but the LH is generally considered important for feeding and reward, and may serve as a potential 'predator attack center' in the brain (O'Connor et al., 2015; Stuber and Wise, 2016; Li et al., 2018). LH OT-ir has been reported in fewer species, but a few scattered OT-ir cells in the LH have been described in Ansell's mole rats (Valesky et al., 2012), Mongolian gerbils (Wang et al., 2013), and Chinese hamsters (Wang et al., 2013). Similar to LH VP, little is known about the role of LH OT-ir in behavior. Interestingly, it appears that spiny mice may exhibit unusually robust VP-ir and OT-ir neuronal populations of the LH.

The presence of VP-ir neurons in the MeA is variable across species. Here we found VP-ir neurons in the MeA, similar to findings that have been reported for rats (De Vries et al., 1985; DiBenedictis et al., 2017), mice (Otero-Garcia et al., 2016; Tong et al., 2020), and jerboas (Lakhdar-Ghazal et al., 1995). However, several species lack VP-ir cells in the MeA, including golden and greater long-tailed hamsters (Ferris et al., 1995; Xu et al., 2010), Ansell's mole rats (Valesky et al., 2012), naked mole rats (Rosen et al., 2008), and Brandt's voles (Xu et al., 2010). The MeA has been consistently implicated in the regulation of defensive behaviors and male sexual behavior (Hull, 2010; Petrulis, 2020). Given the importance of such behaviors to the survival and reproduction of all species, while MeA VP may contribute to defensive and sexual behavior in some species, these behaviors are

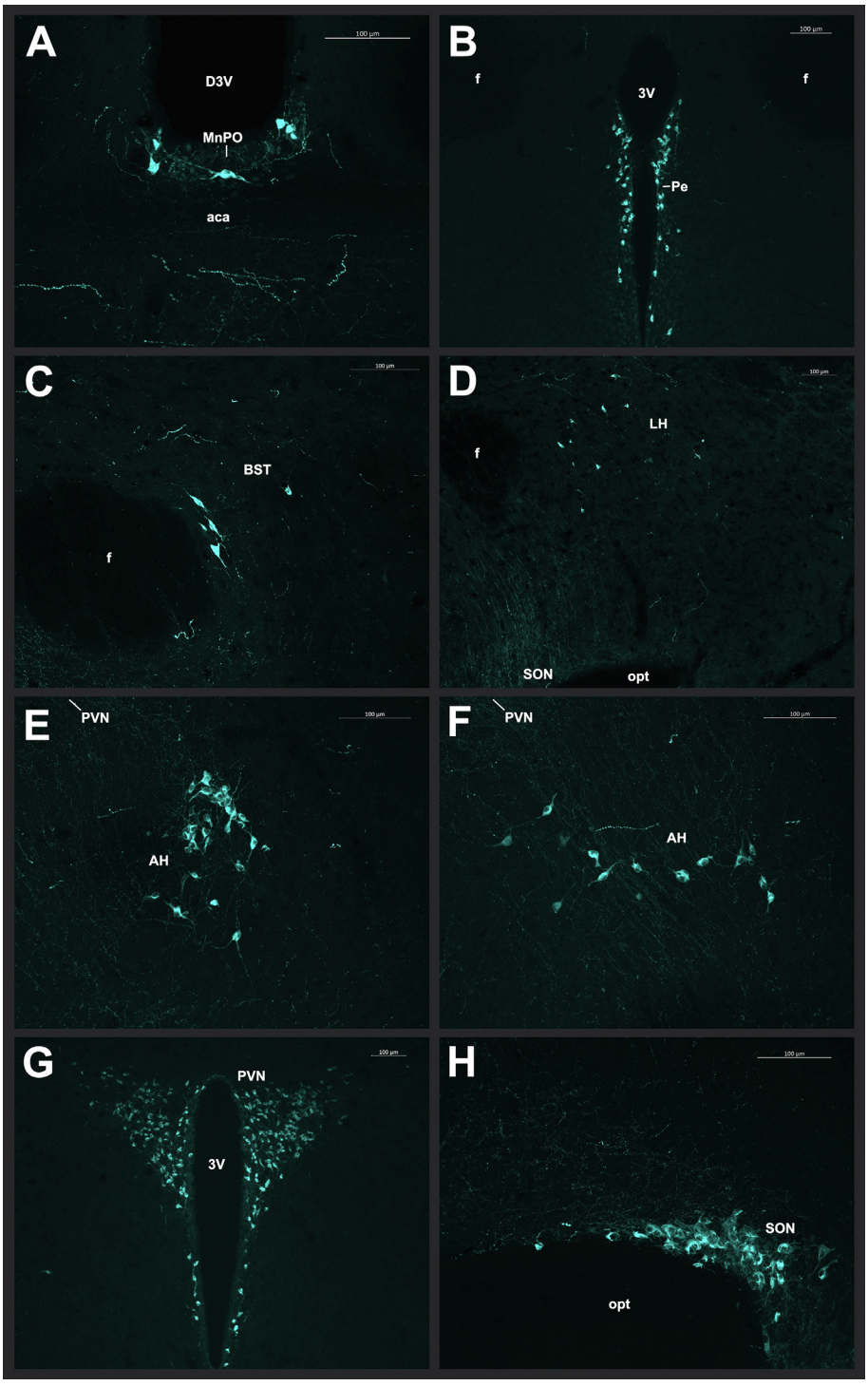

Fig. 6. Photomicrographs of oxytocin-immunoreactive cells: Representative photomicrographs from a male spiny mouse of OT-ir cells in the **(A)** MnPO (20× magnification), **(B)** Pe (10× magnification), **(C)** BST (20× magnification), **(D)** LH (10× magnification), **(E)** rostral AH (20× magnification), **(F)** caudal AH (20× magnification), **(G)** PVN (10× magnification), and **(H)** SON (20× magnification). Images were pseudocolored cyan.

clearly also regulated by systems other than the MeA VP cell group.

Neuroanatomical sex differences in vasopressin and oxytocin neuronal populations

Out of all VP-ir neuronal populations present in the spiny mouse brain, we observed a sex difference only in the VP cell group of the BST. A sexual dimorphism in the BST VP cell group represents one of the largest and most phylogenetically widespread sex differences described in the vertebrate brain (Goodson and Bass, 2001; De Vries and Panzica, 2006; De Vries, 2008; Kelly and Goodson, 2013), and thus spiny mice are no oddity for exhibiting a sex difference in this cell group. Across species, BST VP is strongly regulated by gonadal steroids and males exhibit more VP-ir neurons in the BST compared to females (De Vries et al., 1985). Interestingly, we observed a sex difference in VP-ir cell numbers only in the rostral portion of the BST cell group. This difference has not been described for other species, and thus whether there exists functional delineation within this population remains unknown. Future studies aim to determine whether there is differential axonal targeting in rostral vs. caudal BST VP neurons, which could help elucidate behavioral functions of this morphological sex difference.

Similar to the BST VP cell group, studies in rats have reported a sex difference in MeA VP (males > females), a cell group that is also testosterone dependent (De Vries et al., 1985; Hines et al., 1992; DiBenedictis et al., 2017; Tong et al., 2019). However, we did not observe a sex difference in MeA VP-ir cell numbers in the spiny mice. The function of the BST and MeA VP sex differences is largely thought to be important for male-specific territorial and reproductive behaviors (Ho et al., 2010; Hari Dass and Vyas, 2014; DiBenedictis et al., 2017). Why spiny mice do not exhibit a sex difference in the MeA VP cell group remains unknown, however, it may relate to their breeding system, which is communal and displays low levels of male territoriality (Nowak, 1999; Cizkova et al., 2011; Frynta et al., 2011). A previous study

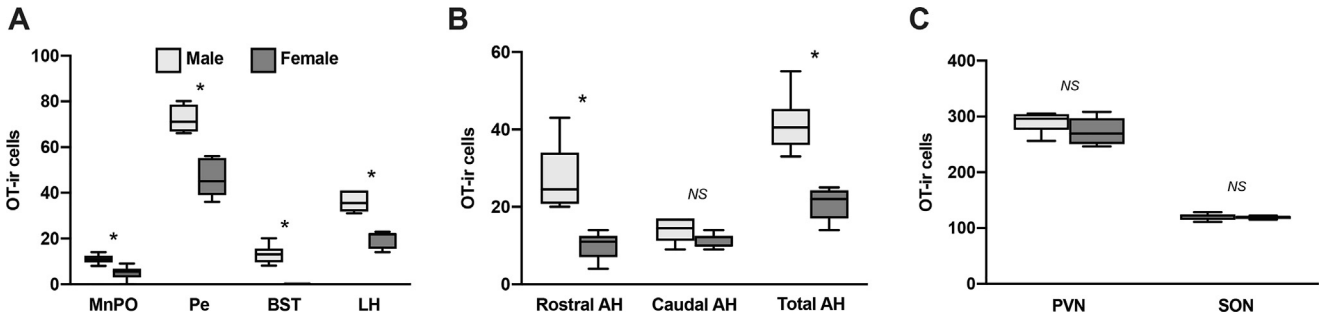

Fig. 7. Effects of sex on the density of oxytocin-immunoreactive cells: Box-and-whisker plots depicting the median, 25th and 75th quartiles, with whiskers showing the 5th and 95th percentile in males (light gray) and females (dark gray) in **(A)** the MnPO, Pe, BST, LH, **(B)** the rostral and caudal portions of the AH, as well as a combined AH measure, and **(C)** the PVN and SON. *Indicates $P < 0.01$. *NS* indicates not statistically significant.

Table 2. Density of oxytocin immunoreactive cells (mean ± SEM) in the brain of male and female African spiny mice. *Indicates $P < 0.01$. *NS* indicates not statistically significant

Brain region	OT-ir cells		Mann Whitney
	Male	Female	
AH Rostral	27.3 ± 3.5	10.0 ± 1.4	*
AH Caudal	14.0 ± 1.3	10.8 ± 0.7	*NS*
AH Combined	41.3 ± 3.0	20.8 ± 1.7	*
BST Rostral	7.0 ± 1.4	0 ± 0	*
BST Caudal	6.0 ± 0.5	0 ± 0	*
BST Combined	13.0 ± 1.7	0 ± 0	*
LH Rostral	17.8 ± 1.4	11.3 ± 1.4	*
LH Caudal	18.2 ± 1.2	9.3 ± 0.7	*
LH Combined	36.0 ± 1.9	19.8 ± 1.6	*
MnPO Rostral	4.6 ± 0.8	1.6 ± 0.7	*
MnPO Caudal	6.3 ± 0.8	3.8 ± 0.8	*
MnPO Combined	11.0 ± 0.8	5.0 ± 1.2	*
Pe Rostral	27.7 ± 1.2	17.8 ± 1.2	*
Pe Caudal	44.5 ± 3.1	28.3 ± 2.6	*
Pe Combined	72.2 ± 2.3	46.2 ± 3.3	*
PVN Rostral	208.8 ± 4.6	200.8 ± 9.8	*NS*
PVN Caudal	81.2 ± 4.8	72.2 ± 3.5	*NS*
PVN Combined	290.0 ± 7.5	273.0 ± 10.0	*NS*
SON Rostral	74.1 ± 2.4	70.0 ± 1.9	*NS*
SON Caudal	46.2 ± 1.8	49.2 ± 1.6	*NS*
SON Combined	120.3 ± 2.4	119.1 ± 1.1	*NS*

in *A. cahirinus* found that female spiny mice are more aggressive than males (Porter, 1976). Similarly, in our lab, we have observed more aggression in all female homecages compared to all male homecages of spiny mice (Kelly et al. *unpub obs.*). Thus, it is possible that the lack of a sex difference in the MeA VP cell group may reflect the unusually low levels of aggression in male spiny mice, thus negating a sex difference in the MeA VP neuronal population.

To our knowledge, only two studies have identified sex differences in OT cell groups outside of the PVN, with female Mandarin voles having more SON and LH OT-ir cells than males (Qiao et al., 2014) and female Mongolian gerbils having more MPO OT-ir cells than males (Wang et al., 2013). In the present study, we found that every OT cell group other than the PVN and SON exhibited a sex difference, with males having significantly more OT-ir neurons than females in the MnPo, Pe, BST, AH, LH, and Pe. Given that OT is primarily involved in promoting prosocial behaviors in many, if not all, contexts (Neumann, 2008; Goodson and Thompson, 2010; Kelly and Goodson, 2014c), it is worth considering that all of the OT-ir cell group sex differences observed here in spiny mice may reflect an evolutionary adaptation that has resulted in spiny mouse males exhibiting an unusually gregarious and prosocial phenotype necessary for the success of a communal breeding system.

Lastly, similar to the potential for functional delineation in the BST VP cell group, we found that the rostral part of the AH OT-ir cell group exhibited a sex difference whereas the caudal portion did not. The rostral AH OT-ir neurons formed a tighter cluster and were located around the nucleus circularis. Notably, the nucleus circularis of the AH in hamsters contains magnocellular VP-ir neurons that are involved flank marking (Ferris et al., 1990). While we do not know the function of this OT-ir sex difference in spiny mice, we can speculate that, again, a robust population of OT-ir neurons in this region

may counteract VP-mediate aggression and territoriality, resulting in higher levels of prosocial behavior in males. Future studies may seek to identify axonal projections of rostral vs. caudal AH OT-ir neurons in an attempt to understand behavioral functions reflected by this anatomical sex difference.

In the present study, we mapped the distribution of OT-ir and VP-ir neurons in the brains of male and female spiny mice and showed that spiny mice exhibit nonapeptide-producing neurons in locations similar to other mammals. We also examined sex differences and confirmed that the BST VP-ir sex difference (males > females) that is phylogenetically widespread across vertebrates also exists in spiny mice. Furthermore, we identified the novel finding of widespread sex differences in oxytocin neurons, such that male spiny mice exhibit significantly more OT-ir neurons than females in both hypothalamic and extra-hypothalamic populations. These results lay a basic foundation for future studies that seek to understand the role of nonapeptides in behavior and physiological processes in spiny mice. Future studies may seek to utilize viral tracing methods for mapping axonal distributions and receptor autoradiography to identify downstream nonapeptide receptor targets.

AUTHOR CONTRIBUTIONS

This collaboration arose from discussions between AMK and AWS about the utility of exploring spiny mice as a potential model for studying sociality and grouping behaviors, as well as relevant underlying neural mechanisms. Spiny mice were provided by AWS. All data collection and analyses were conducted by AMK. The manuscript was written by AMK and AWS.

ACKNOWLEDGEMENTS

We would like to acknowledge funding from the Klingenstein-Simons Foundation (Fellowship Award in Neuroscience to AMK), the National Institute of Mental Health (Emory CONTE Center Pilot Project Grant; P50MH100023 to LJ Young), the National Institute of Arthritis and Musculoskeletal and Skin Diseases (R01AR070313 to AWS) and the National Science Foundation (IOS-1353713 to AWS).

The data that support the findings of this study are available from the corresponding author upon reasonable request.

REFERENCES

Acher R, Chauvet J (1995) The neurohypophysial endocrine regulatory cascade: precursors, mediators, receptors, and effectors. Front Neuroendocrinol 16:237–289.

Albers HE (2012) The regulation of social recognition, social communication and aggression: vasopressin in the social behavior neural network. Horm Behav 61:283–292.

Albers HE, Rowland CM, Ferris CF (1991) Arginine-vasopressin immunoreactivity is not altered by photoperiod or gonadal hormones in the Syrian hamster (*Mesocricetus auratus*). Brain Res 539:137–142.

Alhajeri BH, Hunt OJ, Steppan SJ (2015) Molecular systematics of gerbils and deomyines (Rodentia: Gerbillinae, Deomyinae) and a test of desert adaptation in the tympanic bulla. J Zool Syst Evol Res 53:312–330.

Bellofiore N, Ellery SJ, Mamrot J, Walker DW, Temple-Smith P, Dickinson H, 2017 First evidence of a menstruating rodent: the spiny mouse (Acomys cahirinus) Am J Obstet Gynecol 216, 40 e41-40 e11.

Bellofiore N, Rana S, Dickinson H, Temple-Smith P, Evans J (2018) Characterization of human-like menstruation in the spiny mouse: comparative studies with the human and induced mouse model. Hum Reprod 33:1715–1726.

Bester-Meredith JK, Marler CA (2012) Naturally occurring variation in vasopressin immunoreactivity is associated with maternal behavior in female peromyscus mice. Brain Behav Evol 80:244–253.

Bosch OJ (2011) Maternal nurturing is dependent on her innate anxiety: the behavioral roles of brain oxytocin and vasopressin. Horm Behav 59:202–212.

Brunjes PC (1985) A stereological study of neocortical maturation in the precocial mouse. Acomys cahirinus Brain Res 351:279–287.

Brunjes PC (1990) The precocial mouse, Acomys cahirinus. Psychobiology 18:339–350.

Brunjes PC, Korol DL, Stern KG (1989) Prenatal neurogenesis in the telencephalon of the precocial mouse Acomys cahirinus. Neurosci Lett 107:114–119.

Cizkova B, Sumbera R, Frynta D (2011) A new member or an intruder: how do Sinai spiny mouse (*Acomys dimidiatus*) families respond to a male newcomer? Behaviour 148:889–908.

De Vries GJ (2008) Sex differences in vasopressin and oxytocin innervation of the brain. Prog Brain Res 170:17–27.

De Vries GJ, Buijs RM, Van Leeuwen FW, Caffe AR, Swaab DF (1985) The vasopressinergic innervation of the brain in normal and castrated rats. J Comp Neurol 233:236–254.

De Vries GJ, Panzica GC (2006) Sexual differentiation of central vasopressin and vasotocin systems in vertebrates: different mechanisms, similar endpoints. Neuroscience 138:947–955.

Deacon RM (2009) Burrowing: a sensitive behavioural assay, tested in 5 species of laboratory rodents. Behav Brain Res 200:128–133.

DiBenedictis BT, Nussbaum ER, Cheung HK, Veenema AH (2017) Quantitative mapping reveals age and sex differences in vasopressin, but not oxytocin, immunoreactivity in the rat social behavior neural network. J Comp Neurol.

Dogterom J, Snijdewint FG, Buijs RM (1978) The distribution of vasopressin and oxytocin in the rat brain. Neurosci Lett 9:341–346.

Donaldson ZR, Young LJ (2008) Oxytocin, vasopressin, and the neurogenetics of sociality. Science 322:900–904.

Dubois-Dauphin M, Pevet P, Tribollet E, Dreifuss JJ (1990) Vasopressin in the brain of the golden hamster: the distribution of vasopressin binding sites and of immunoreactivity to the vasopressin-related glycopeptide. J Comp Neurol 300:535–548.

Duque-Wilckens N, Torres LY, Yokoyama S, Minie VA, Tran AM, Petkova SP, Hao R, Ramos-Maciel S, Rios RA, Jackson K, Flores-Ramirez FJ, Garcia-Carachure I, Pesavento PA, Iniguez SD, Grinevich V, Trainor BC (2020) Extrahypothalamic oxytocin neurons drive stress-induced social vigilance and avoidance. Proc Natl Acad Sci U S A 117:26406–26413.

Fabre PH, Hautier L, Dimitrov D, Douzery EJP (2012) A glimpse on the pattern of rodent diversification: a phylogenetic approach. BMC Evol Biol:12.

Ferris CF, Delville Y, Miller MA, Dorsa DM, De Vries GJ (1995) Distribution of small vasopressinergic neurons in golden hamsters. J Comp Neurol 360:589–598.

Ferris CF, Gold L, De Vries GJ, Potegal M (1990) Evidence for a functional and anatomical relationship between the lateral septum and the hypothalamus in the control of flank marking behavior in Golden hamsters. J Comp Neurol 293:476–485.

Fluxman S, Haim A (1993) Daily rhythms of body temperature in Acomys russatus: the response to chemical signals released by Acomys cahirinus. Chronobiol Int 10:159–164.

Frynta D, Frankova M, Cizkova B (2011) Social and life history correlates of litter size in captive colonies of precocial spiny mice (*Acomys*). Acta Theriol 56:289–295.
Gawriluk TR, Simkin J, Thompson KL, Biswas SK, Clare-Salzler Z, Kimani JM, Kiama SG, Smith JJ, Ezenwa VO, Seifert AW (2016) Comparative analysis of ear-hole closure identifies epimorphic regeneration as a discrete trait in mammals. Nat Commun 7:11164.
Gobrogge KL, Liu Y, Young LJ, Wang Z (2009) Anterior hypothalamic vasopressin regulates pair-bonding and drug-induced aggression in a monogamous rodent. Proc Natl Acad Sci U S A 106:19144–19149.
Gonet AE, Stauffacher W, Pictet R, Renold AE (1966) Obesity and diabetes mellitus with striking congenital hyperplasia of the islets of langerhans in spiny mice (Acomys Cahirinus): I. Histological findings and preliminary metabolic observations. Diabetologia 1:162–171.
Goodson JL, Bass AH (2001) Social behavior functions and related anatomical characteristics of vasotocin/vasopressin systems in vertebrates. Brain Res Rev 35:246–265.
Goodson JL, Thompson RR (2010) Nonapeptide mechanisms of social cognition, behavior and species-specific social systems. Curr Opin Neurobiol 20:784–794.
Grimes JM, Ricci LA, Melloni RHJ (2007) Alterations in anterior hypothalamic vasopressin, but not serotonin, correlate with temporal onset of aggressive behavior during adolescent anabolic-androgenic steroid exposure in hamsters (Mesocricetus auratus). Behav Neurosci 121:941–948.
Gutman R, Dayan T, Temporal partitioning: an experiment with two species of spiny mice. Ecology 86, 164–173.
Hari Dass SA, Vyas A (2014) Copulation or sensory cues from the female augment Fos expression in arginine vasopressin neurons of the posterodorsal medial amygdala of male rats. Front Zool 11:42.
Harmon AC, Huhman KL, Moore TO, Albers HE (2002) Oxytocin inhibits aggression in female Syrian hamsters. J Neuroendocrinol 14:963–969.
Hastings MH, Maywood ES, Brancaccio M (2018) Generation of circadian rhythms in the suprachiasmatic nucleus. Nat Rev Neurosci 19:453–469.
Haughton CL, Gawriluk TR, Seifert AW (2016) The biology and husbandry of the African Spiny Mouse (*Acomys cahirinus*) and the research uses of a laboratory colony. J Am Assoc Lab Anim Sci 55:9–17.
Hines M, Allen LS, Gorski RA (1992) Sex differences in subregions of the medial nucleus of the amygdala and the bed nucleus of the stria terminalis of the rat. Brain Res 579:321–326.
Ho JM, Murray JH, Demas GE, Goodson JL (2010) Vasopressin cell groups exhibit strongly divergent responses to copulation and male-male interactions in mice. Horm Behav 58:368–377.
Hoyle CHV (1998) Neuropeptide families: evolutionary perspectives. Regul Pept 73:1–33.
Hull EM (2010) Male sexual behavior. Encyclopedia of Behavioral Neuroscience Academic Press:154–162.
Jackson D, Burns R, Trksak G, Simeone B, DeLeon KR, Connor DF, Harrison RJ, Melloni Jr RH (2005) Anterior hypothalamic vasopressin modulates the aggression-stimulating effects of adolescent cocaine exposure in Syrian hamsters. Neuroscience 133:635–646.
Kelly AM, Goodson JL (2013) Functional significance of a phylogenetically widespread sexual dimorphism in vasotocin/vasopressin production. Horm Behav 64:840–846.
Kelly AM, Goodson JL (2014a) Hypothalamic oxytocin and vasopressin neurons exert sex-specific effects on pair bonding, gregariousness and aggression in finches. Proc Natl Acad Sci U S A 111:6069–6074.
Kelly AM, Goodson JL (2014b) Personality is tightly coupled to vasopressin-oxytocin neuron activity in a gregarious finch. Front Behav Neurosci:8.
Kelly AM, Goodson JL (2014c) Social functions of individual vasopressin-oxytocin cell groups in vertebrates: What do we really know? Front Neuroendocrinol 35:512–529.
Kelly AM, Hiura LC, Ophir AG (2018a) Rapid nonapeptide synthesis during a critical period of development in the prairie vole: plasticity of the paraventricular nucleus of the hypothalamus. Brain Struct Funct 223:2547–2560.
Kelly AM, Hiura LC, Saunders AG, Ophir AG (2017) Oxytocin neurons exhibit extensive functional plasticity due to offspring age in mothers and fathers. Integr Comp Biol 57:603–618.
Kelly AM, Kingsbury MA, Hoffbuhr K, Schrock SE, Waxman B, Kabelik D, Thompson RR, Goodson JL (2011) Vasotocin neurons and septal V_{1a}-like receptors potently modulate songbird flocking and responses to novelty. Horm Behav 60:12–21.
Kelly AM, Saunders AG, Ophir AG (2018b) Mechanistic substrates of a life history transition in male prairie voles: Developmental plasticity in affiliation and aggression corresponds to nonapeptide neuronal function. Horm Behav 99:14–24.
Lakhdar-Ghazal N, Dubois-Dauphin M, Hermes ML, Buijs RM, Bengelloun WA, Pevet P (1995) Vasopressin in the brain of a desert hibernator, the jerboa (*Jaculus orientalis*): presence of sexual dimorphism and seasonal variation. J Comp Neurol 358:499–517.
Landgraf R, Neumann ID (2004) Vasopressin and oxytocin release within the brain: a dynamic concept of multiple and variable modes of neuropeptide communication. Front Neuroendocrinol 25:150–176.
Lee AG, Cool DR, Grunwald Jr WC, Neal DE, Buckmaster CL, Cheng MY, Hyde SA, Lyons DM, Parker KJ (2011) A novel form of oxytocin in New World monkeys. Biol Lett 7:584–587.
Lee NS, Goodwin NL, Freitas KE, Beery AK (2019) Affiliation, aggression, and selectivity of peer relationships in meadow and prairie voles. Front Behav Neurosci 13:52.
Li Y, Zeng J, Zhang J, Yue C, Zhong W, Liu Z, Feng Q, Luo M (2018) Hypothalamic circuits for predation and evasion. Neuron 97:911–924 e915.
Lowry CA, Richardson CF, Zoeller TR, Miller LJ, Muske LE, Moore FL (1997) Neuroanatomical distribution of vasotocin in a urodele amphibian (*Taricha granulosa*) revealed by immunohistochemical and in situ hybridization techniques. J Comp Neurol 385:43–70.
McKinley MJ, Yao ST, Uschakov A, McAllen RM, Rundgren M, Martelli D (2015) The median preoptic nucleus: front and centre for the regulation of body fluid, sodium, temperature, sleep and cardiovascular homeostasis. Acta Physiol (Oxf) 214:8–32.
Moore FL, Lowry CA (1998) Comparative neuroanatomy of vasotocin and vasopressin in amphibians and other vertebrates. Comp Biochem Physiol C Pharmacol Toxicol Endocrinol 119:251–260.
NCfB, (2020a) PubChem Compound Summary for CID 439302, Oxytocin Retrieved fromAvailable from: https://pubchem.ncbi.nlm.nih.gov/compound/Oxytocin, 2020.
NCfB, (2020b) PubChem Compound Summary for CID 53481539, Arginine vasopressin 1–8 Retrieved fromAvailable from: https://pubchem.ncbi.nlm.nih.gov/compound/Arginine-vasopressin-1-8, 2020.
Neumann ID (2008) Brain oxytocin: a key regulator of emotional and social behaviours in both females and males. J Neuroendocrinol 20:858–865.
Ni RJ, Shu YM, Wang J, Yin JC, Xu L, Zhou JN (2014) Distribution of vasopressin, oxytocin and vasoactive intestinal polypeptide in the hypothalamus and extrahypothalamic regions of tree shrews. Neuroscience 265:124–136.
Nowak RM (1999) Walker's mammals of the world. Baltimore (MD): John Hopkins University Press.
O'Connor EC, Kremer Y, Lefort S, Harada M, Pascoli V, Rohner C, Luscher C (2015) Accumbal D1R neurons projecting to lateral hypothalamus authorize feeding. Neuron 88:553–564.
Otero-Garcia M, Agustin-Pavon C, Lanuza E, Martinez-Garcia F (2016) Distribution of oxytocin and co-localization with arginine vasopressin in the brain of mice. Brain Struct Funct 221:3445–3473.
Pan Y, Zhu Q, Xu T, Zhang Z, Wang Z (2020) Aggressive behavior and brain neuronal activation in sexually naive male Mongolian gerbils. Behav Brain Res 378 112276.

Paxinos G, Watson C, Carrive P, Kirkcaldie MTK, Ashwell K, 2009 Chemoarchitectonic atlas of the rat brain.
Petrulis A, 2020, Chapter 2 - Structure and function of the medial amygdala. Handbook of Behavioral Neuroscience 26, 39–61.
Porter RH (1976) Sex-differences in the agonistic behavior of spiny mice (Acomys cahirinus). Z Tierpsychol 40:100–108.
Prasada Rao PD, Kanwal JS (2004) Oxytocin and vasopressin immunoreactivity within the forebrain and limbic-related areas in the mustached bat, *Pteronotus parnellii*. Brain Behav Evol 63:151–168.
Qiao X, Yan Y, Wu R, Tai F, Hao P, Cao Y, Wang J (2014) Sociality and oxytocin and vasopressin in the brain of male and female dominant and subordinate mandarin voles. J Comp Physiol A 200:149–159.
Rigney N, Whylings J, Mieda M, de Vries G, Petrulis A 2019 Sexually dimorphic vasopressin cells modulate social investigation and communication in sex-specific ways eNeuro 6.
Rood BD, De Vries GJ (2011) Vasopressin innervation of the mouse (*Mus musculus*) brain and spinal cord. J Comp Neurol 519:2434–2474.
Rosen GJ, De Vries GJ, Goldman SL, Goldman BD, Forger NG (2007) Distribution of vasopressin in the brain of the eusocial naked mole-rat. J Comp Neurol 500:1093–1105.
Rosen GJ, de Vries GJ, Goldman SL, Goldman BD, Forger NG (2008) Distribution of oxytocin in the brain of a eusocial rodent. Neuroscience 155:809–817.
Rosen GJ, De Vries GJ, Villalba C, Weldele ML, Place NJ, Coscia EM, Glickman SE, Forger NG (2006) Distribution of vasopressin in the forebrain of spotted hyenas. J Comp Neurol 498:80–92.
Ruan C, Zhang Z (2016) Laboratory domestication changed the expression patterns of oxytocin and vasopressin in brains of rats and mice. Anat Sci Int 91:358–370.
Schoepf I, Kenkel W, Schradin C (2015) Arginine vasopressin in brains of free ranging striped mouse males following alternative reproductive tactics. J Ethol 33:235–242.
Schradin C, Drouard F, Lemonnier G, Askew R, Olivier CA, Pillay N (2020) Geographic intra-specific variation in social organization is driven by population density. Behav Ecol Sociobiol:74.
Seifert AW, Kiama SG, Seifert MG, Goheen JR, Palmer TM, Maden M (2012) Skin shedding and tissue regeneration in African spiny mice (*Acomys*). Nature 489:561–565.
Shafrir E (2000) Overnutrition in spiny mice (Acomys cahirinus): beta-cell expansion leading to rupture and overt diabetes on fat-rich diet and protective energy-wasting elevation in thyroid hormone on sucrose-rich diet. Diabetes Metab Res Rev 16:94–105.
Shi H, Bartness TJ (2000) Catecholaminergic enzymes, vasopressin and oxytocin distribution in Siberian hamster brain. Brain Res Bull 53:833–843.
Simmons DA, Yahr P (2011) Distribution of catecholaminergic and peptidergic cells in the gerbil medial amygdala, caudal preoptic area and caudal bed nuclei of the stria terminalis with a focus on areas activated at ejaculation. J Chem Neuroanat 41:13–19.
Steppan SJ, Schenk JJ (2017) Muroid rodent phylogenetics: 900-species tree reveals increasing diversification rates. Plos One 12.
Stuber GD, Wise RA (2016) Lateral hypothalamic circuits for feeding and reward. Nat Neurosci 19:198–205.
Tong WH, Abdulai-Saiku S, Vyas A (2019) Testosterone reduces fear and causes drastic hypomethylation of arginine vasopressin promoter in medial extended amygdala of male mice. Front Behav Neurosci 13:33.
Tong WH, Abdulai-Saiku S, Vyas A (2020) Medial amygdala arginine vasopressin neurons regulate innate aversion to cat odors in male mice. Neuroendocrinology.
Tuckova V, Sumbera R, Cizkova B (2016) Alloparental behaviour in Sinai spiny mice (*Acomys dimidiatus*): a case of misdirected parental care? Behav Ecol Sociobiol 70:437–447.
Valesky EM, Burda H, Kaufmann R, Oelschlager HHA (2012) Distribution of oxytocin- and vasopressin- immunoreactive neurons in the brain of the eusocial mole rat (*Fukomys anselli*). Anat Rec 295:474–480.
Van der Zee EA, Jansen K, Gerkema MP (1999) Severe loss of vasopressin-immunoreactive cells in the suprachiasmatic nucleus of aging voles coincides with reduced circadian organization of running wheel activity. Brain Res 816:572–579.
Vandesande F, Dierickx K, DeMey J (1975) Identification of the vasopressin-neurophysin producing neurons of the rat suprachiasmatic nuclei. Cell Tissue Res 156:377–380.
Wang Y, Xu L, Pan Y, Wang Z, Zhang Z (2013) Species differences in the immunoreactive expression of oxytocin, vasopressin, tyrosine hydroxylase and estrogen receptor alpha in the brain of Mongolian gerbils (Meriones unguiculatus) and Chinese striped hamsters (Cricetulus barabensis). PLoS One 8 e65807.
Wang Z (1995) Species differences in the vasopressin-immunoreactive pathways in the bed nucleus of the stria terminalis and medial amygdaloid nucleus in prairie voles (*Microtus ochrogaster*) and meadow voles (*Microtus pennsylvanicus*). Behav Neurosci 109:305–311.
Wang Z, Zhou L, Hulihan TJ, Insel TR (1996) Immunoreactivity of central vasopressin and oxytocin pathways in microtine rodents: a quantitative comparative study. J Comp Neurol 366:726–737.
Whitman DC, Albers HE (1998) Oxytocin immunoreactivity in the hypothalamus of female hamsters. Cell Tissue Res 291:231–237.
Xu L, Pan Y, Young KA, Wang Z, Zhang Z (2010) Oxytocin and vasopressin immunoreactive staining in the brains of Brandt's voles (Lasiopodomys brandtii) and greater long-tailed hamsters (Tscherskia triton). Neuroscience 169:1235–1247.
Yu P, Zhang M, Nan X, Zhao H, Gong D (2020) Differences in the number of oxytocin, vasopressin, and tyrosine hydroxylase cells in brain regions associated with mating among great, midday, and Mongolian gerbils. Brain Res 1733 146677.

(Received 10 March 2021, Accepted 28 May 2021)
(Available online 05 June 2021)